

# Mitoxantrone removal by electrochemical method: A comparison of homogenous and heterogenous catalytic reactions

Abbas Jafarizad<sup>1</sup>, Mohammad Rostamizadeh<sup>2\*</sup>, Mahmoud Zarei<sup>3</sup>, Soorena Gharibian<sup>1</sup>

<sup>1</sup>Department of Chemical Engineering, School of Chemistry, Sahand University of Technology, Tabriz, Iran

<sup>2</sup>Department of Chemical Engineering, School of Environment, Sahand University of Technology, Tabriz, Iran

<sup>3</sup>Department of Applied Chemistry, School of chemistry, University of Tabriz, Tabriz, Iran

## Abstract

**Background:** Mitoxantrone (MXT) is a drug for cancer therapy and a hazardous pharmaceutical to the environment which must be removed from contaminated waste streams. In this work, the removal of MXT by the electro-Fenton process over heterogeneous and homogenous catalysts is reported.

**Methods:** The effects of the operational conditions (reaction medium pH, catalyst concentration and utilized current intensity) were studied. The applied electrodes were carbon cloth (CC) without any processing (homogenous process), graphene oxide (GO) coated carbon cloth (GO/CC) (homogenous process) and Fe<sub>3</sub>O<sub>4</sub>@GO nanocomposite coated carbon cloth (Fe<sub>3</sub>O<sub>4</sub>@GO/CC) (heterogeneous process). The characteristic properties of the electrodes were determined by atomic force microscopy (AFM), field emission scanning electron microscopy (FE-SEM) and cathode polarization. MXT concentrations were determined by using ultraviolet-visible (UV-Vis) spectrophotometer.

**Results:** In a homogenous reaction, the high concentration of Fe catalyst (>0.2 mM) decreased the MXT degradation rate. The results showed that the Fe<sub>3</sub>O<sub>4</sub>@GO/CC electrode included the most contact surface. The optimum operational conditions were pH 3.0 and current intensity of 450 mA which resulted in the highest removal efficiency (96.9%) over Fe<sub>3</sub>O<sub>4</sub>@GO/CC electrode in the heterogeneous process compared with the other two electrodes in a homogenous process. The kinetics of the MXT degradation was obtained as a pseudo-first order reaction.

**Conclusion:** The results confirmed the high potential of the developed method to purify contaminated wastewaters by MXT.

**Keywords:** Mitoxantrone, Electrodes, Nanocomposite, Organic chemicals, Carbon

**Citation:** Jafarizad A, Rostamizadeh M, Zarei M, Gharibian S. Mitoxantrone removal by electrochemical method: A comparison of homogenous and heterogenous catalytic reactions. Environmental Health Engineering and Management Journal 2017; 4(4): 185–193. doi: 10.15171/EHEM.2017.26.

## Article History:

Received: 24 April 2017

Accepted: 6 August 2017

ePublished: 25 August 2017

## \*Correspondence to:

Mohammad Rostamizadeh

Email: Rostamizadeh@sut.ac.ir

## Introduction

Nowadays, the importance of water pollution is highly critical to people, scientists and governments. The occurrence of global warming, melting glaciers, evaporation of surface waters and increased water consumption by humans can be attributed to this problem (1). Industries are a huge source of wastewater production while hazardous wastewater results in health risks for humans and pollution issues for the environment (2). The pharmaceutical industry is among industries which produce wastewater including pharmaceuticals as hazardous waste. The lack of required technology or high costs of wastewater treatments and also the low removal efficiency of waste water treatment plants (WWTPs) on pharmaceuticals compounds (3-5) lead to the discharge

of these wastewaters into the environment (6). Hence, it is necessary to study the new low cost methods for wastewater treatment. To avoid the dangerous accumulation of organic materials in the environment, it is necessary to develop effective methods for the degradation of such organic pollutants (7). The current treatment methods for the wastewater of pharmaceutical industries are: (i) chemical precipitation which requires a large amount of chemicals and has other drawbacks such as sludge production, aggregation of precipitates and issues of sludge disposal (8), (ii) evaporation which requires high initial investment and large land requirements (9), (iii) solvent extraction while most of the solvents are not selective enough, (iv) ion exchange which has concentration limits and resin bed fouling problems, and (v) reverse osmosis and



membrane separation which generally are not selective enough and have fouling as well as short membrane life time problems (7).

So far, various treatment methods such as ozonation and filtration with granular activated carbon (GAC) (8) have been investigated for the efficient removal of pharmaceuticals from water. Also, advanced oxidation processes (AOPs) which basically includes the *in situ* generation of hydroxyl radicals ( $\text{OH}^\bullet$ ) have shown a promising potential (10). AOPs include ozonation, catalytic ozonation, ultrasonication, Fenton and Fenton like reactions as well as hybrid methods which include less disadvantages, less investment and relatively low maintenance costs compared with the conventional methods of wastewater purification (10). The electro-Fenton process is one of the frequently investigated AOP methods and it is a catalytic process. The electro-Fenton process can be carried out both homogeneously and heterogeneously. Heterogeneous processes have the advantage of a reusable catalyst. The catalyst includes Fe species over support which can be the electrode itself or introduced in the reaction medium as solid particles (11-15).

In the AOP process, the required reactants ( $\text{H}_2\text{O}_2$  and  $\text{Fe}^{2+}$ ) to conduct Fenton's reaction are electrochemically produced in the reaction medium through the following reactions (Eq. 1-4).

Reduction of dissolved oxygen to form hydrogen peroxide:

$$\text{O}_2 + 2\text{H}^+ + 2\text{e}^- \rightarrow \text{H}_2\text{O}_2 \quad (1)$$

Reduction of ferric ( $\text{Fe}^{3+}$ ) ions to ferrous ( $\text{Fe}^{2+}$ ) ions:

$$\text{Fe}^{3+} + \text{e}^- \rightarrow \text{Fe}^{2+} \quad (2)$$

Reaction of  $\text{H}_2\text{O}_2$  and  $\text{Fe}^{2+}$  to form hydroxyl radical and  $\text{Fe}^{3+}$ :

$$\text{Fe}^{2+} + \text{H}_2\text{O}_2 + \text{H}^+ \rightarrow \text{Fe}^{3+} + \text{H}_2\text{O}_2 + \text{OH}^\bullet \quad (3)$$

Oxidation of water on the anode surface to form molecular oxygen (16):

$$2\text{H}_2\text{O} \rightarrow \text{O}_2 + 4\text{H}^+ + 4\text{e}^- \quad (4)$$

The hydroxyl radicals formed are strong oxidants and attack organic pollutants (MXT) and it causes degradation of pollutants (Eq. 5).

$$\text{MXT} + \text{OH}^\bullet \rightarrow \text{degradation of the MXT} \quad (5)$$

The heterogeneous electro-Fenton process mechanism is similar to the above mechanism and is conducted on an electrode surface. Shen et al and Zhao et al have extensively determined the mechanism of the heterogeneous electro-Fenton process conducted with a composite cathode (17,18).

It has been reported that the cathode materials directly influence the electro-Fenton process through  $\text{H}_2\text{O}_2$  production. The efficiency of materials such as graphite felt, carbon nanotube, active carbon, stainless steel, platinum, titanium and boron doped diamond were investigated in the electro-Fenton process (19,20).

The spectacular magnetic properties in the form of permanent magnetization and Fe content in both divalent and trivalent states (21,22) resulted in the application of

$\text{Fe}_3\text{O}_4$  NPs in various fields such as medical, drug delivery systems (DDSs), magnetic resonance imaging (MRI), cancer therapy and microwave devices, magneto-optics devices, sensors, high frequency applications, catalysis, magnetic sensing as well as Fenton and Fenton like processes (17,23,24).

The properties of graphene oxide (GO) are easy functionalization, electrical insulator, the large specific surface area and easy dispersion in water and other organic solvents owing to the presence of oxygen functionalities (25). Several studies have reported the use of graphene for anchoring  $\text{Fe}_3\text{O}_4$  to degrade the organic pollutants by the Fenton-like reaction (26,27).

$\text{Fe}_3\text{O}_4$ @GO nanocomposite has many favored properties such as considerably high saturation magnetization, interesting electronic transport properties, low toxicity, bio-compatibility, availability of hydroxyl, epoxy and carbocyclic acid groups. Therefore, it would be a very excellent platform for the generation of a new type of composites as electrode in the electro-Fenton like processes (26,28).

Mitoxantrone (MXT) is a synthetic antineoplastic drug structurally analogous to anthracyclines such as doxorubicin (DOX). MXT has been used in the treatment of various cancers including leukemia, non-Hodgkin lymphoma and breast cancer (29).

To the best of our knowledge, there is no report related to the degradation of MXT by the electro-Fenton process. Therefore, the main aim of this study was to develop a cathode using  $\text{Fe}_3\text{O}_4$  nanoparticles and GO properties with the higher surface area which promotes  $\text{H}_2\text{O}_2$  production rate and the ability of the electro-Fenton reaction to remove MXT. Furthermore, the effect of different operational conditions such as pH, catalyst concentration and applied current intensity were investigated.

## Materials and Methods

### Materials

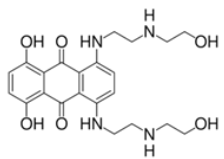
MXT (Sigma Aldrich, R&D grade) was chosen as the model compound and utilized without further purification. Analytical grade n-butanol, graphite, DiMethyl Formamide (DMF),  $\text{FeSO}_4$  and  $\text{Na}_2\text{SO}_4$  were obtained from Merck. Carbon cloth (CC) was purchased from Pars Hydro Pasargad, Iran. All experiments were carried out in deionized water.

An aqueous solution of MXT is blue and absorbs visible light at a wavelength of 630 nm (30). Hence, by determining its absorbance through the use of ultra violet-visible (UV-Vis) technique, it would be possible to determine its concentration in water using a calibration curve. Table 1 shows the MXT properties.

### Characterization

Characteristic properties such as summits density, surface morphology and removal efficiency in both heterogeneous and homogeneous processes were

**Table 1.** General information on MXT

Structure	Formula	Molar Mass	$\lambda_{\max}$
	$C_{22}H_{28}N_4O_6$	444.481 gmol <sup>-1</sup>	630 nm

determined by AFM (Nanosurf mobile S, Switzerland) and FE-SEM (Tescan Mira3 field emission device, Czech). The concentration of the mentioned drug in the sample after the treatment process was determined by using UV-Vis spectrophotometer (UV 1700 Shimadzu UV-Vis spectrophotometer, Japan). The solution pH was measured with a Metrohm 654 pH-meter, Switzerland. Current intensity–potential curves were plotted by cyclic voltammetry using a conventional three-electrode cell in conjunction with a computer controlled multichannel potentiostat (PG-Stat 30, the Netherland) with a scan rate equal to 10 mVs<sup>-1</sup>.

#### Synthesis of graphene oxide

0.3 g of graphite and 0.01 mg of sodium nitrate were added to 50 mL of sulfuric acid at room temperature (25°C) and agitated for 10 minutes. The solution was placed in an ice-water bath at 4°C. KMnO<sub>4</sub> (6 g) was slowly added to the solution and agitated for 30 minutes. The mixture was placed in an oil bath at 35°C and agitated for 3 hours until the color of the solution turned into brown. Once again, the solution was placed in an ice-water bath at 4°C and an appropriate amount of water was added. The solution temperature was raised to 80°C. After reaction for 15 minutes, the temperature was controlled till it reached 40°C. After 30 minutes, a certain amount of water was added to the mixture and hydrogen peroxide was drop-wisely added to the resulted solution until the solution became yellowish. At the final step, the mixture was filtered, washed by deionized water and dried in oven at 80°C (27).

#### Synthesis of Fe<sub>3</sub>O<sub>4</sub> nanoparticles

Tris (acetylacetonato) iron (III) (Fe(acac)<sub>3</sub>, 1.06 g) was dissolved in a mixture of oleylamine (15 mL) and benzyl ether (15 mL) in a four-necked round bottom glass reactor under continuous stirring. The mixture was heated to 120°C and kept at this temperature for 1 hour to remove the humidity under a flow of nitrogen gas. There was continuous stirring during all steps of the reaction. Then, the temperature of the mixture was rapidly increased to 300°C and the reaction was continued for 1 hour at this temperature. Finally, the mixture was separated into two centrifuge tubes including 40 mL of ethanol and centrifuged at 8500 rpm for 12 minutes. After the purification of Fe<sub>3</sub>O<sub>4</sub> nanoparticles, the nanoparticles were dispersed in hexane and saved for further use (28).

#### Synthesis of Fe<sub>3</sub>O<sub>4</sub>@GO nanocomposites

Twelve milligrams amount of Fe<sub>3</sub>O<sub>4</sub> nanoparticles was dispersed in chloroform and added into a round bottom flask containing 12 mg GO suspension in DMF. The GO-Fe<sub>3</sub>O<sub>4</sub> solution was sonicated at room temperature for 3 hours. The Fe<sub>3</sub>O<sub>4</sub>@GO nanocomposites were separated using a magnet. Finally, Fe<sub>3</sub>O<sub>4</sub>@GO nanocomposites were dispersed in 40 mL of *n*-hexane and centrifuged at 7500 rpm for 10 minutes, followed by drying under vacuum (28).

#### Preparation of GO/CC and Fe<sub>3</sub>O<sub>4</sub>@GO/CC electrodes

0.1 g GO or Fe<sub>3</sub>O<sub>4</sub>/GO, deionized water (60 mL) and *n*-butanol (3%) were mixed in an ultrasonic bath (Grant, England) for 10 minutes to form a highly dispersed mixture. The resulting mixture was heated at 80°C until it resembled an ointment in appearance. The ointment was bonded to a CC and sintered at 350°C for 30 minutes under inert conditions (N<sub>2</sub>).

#### Electro-Fenton process

All experiments were conducted at the ambient temperature (25°C) in an open, undivided cell (250 mL beaker) whose cathode (prepared electrodes) and anode (graphite) were hung up to the edges of the beaker including a DC power supply (Figure 1). The initial concentration of the MXT drug (C<sub>0</sub>) was 5 mg/L and ambient air was injected to the beaker while the reaction medium was continuously stirred. The process of CC and GO/CC electrodes were

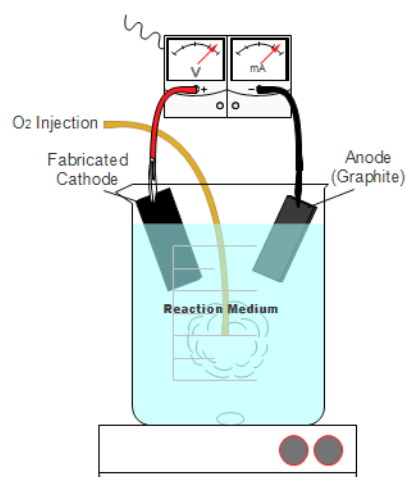


**Figure 1.** The experimental setup used in the electro-Fenton process.

homogenous and Fe catalyst was dispersed in the reaction medium by dissolving  $\text{FeSO}_4$ . The process of  $\text{Fe}_3\text{O}_4@\text{GO}/\text{CC}$  electrode was heterogeneous and thereby no amount of  $\text{FeSO}_4$  catalyst was dissolved in the reaction medium.

## Results

Figure 2 presents the FE-SEM images of CC, GO/CC and  $\text{Fe}_3\text{O}_4@\text{GO}/\text{CC}$  electrodes surface. It was observed that coatings on the CC increased the contact surface while the  $\text{Fe}_3\text{O}_4@\text{GO}/\text{CC}$  electrode showed the most contact surface among the two other electrodes. These results are consistent with the AFM results.

The AFM results (Figure 3) represent the provided contact surface by electrodes. The summits were in the following order:  $\text{Fe}_3\text{O}_4@\text{GO}/\text{CC} > \text{GO}/\text{CC} > \text{CC}$ . The high contact surface enhanced the pollutant elimination by means of more produced  $\text{H}_2\text{O}_2$ . It is obvious that  $\text{Fe}_3\text{O}_4@\text{GO}/\text{CC}$  had more active sites for the generation of  $\text{H}_2\text{O}_2$  than other used cathodes. Therefore, increasing the surface area for this electrode led to an increase in the electrogeneration of  $\text{H}_2\text{O}_2$ . According to these results, it can be concluded that  $\text{Fe}_3\text{O}_4@\text{GO}/\text{CC}$  is a good cathode for the electrogeneration of  $\text{H}_2\text{O}_2$ .

For a given electrical potential, the  $\text{Fe}_3\text{O}_4@\text{GO}/\text{CC}$  electrode released more current intensity than the GO/CC electrode which released higher current intensity compared with the CC electrode (Figure 4). It is clear that the increased current intensity provided more  $\text{H}_2\text{O}_2$  which led to the elimination of more pollutants.

## Discussion

### MXT degradation rate constant

The rate of reaction could be written as second order (Eq.

6) or as a pseudo-first order (Eq. 7) (16) due to the steady-state concentration of hydroxyl.

$$\frac{1}{C} = \frac{1}{C_0} + k_{app}t \quad (6)$$

$$\ln(C/C_0) = -k_{app}t \quad (7)$$

The obtained data for MXT concentration were well fitted in Eq. 7 and so MXT degradation can be compared under different operating parameters using the slope of curves in Figures 5-7 as pseudo-first order rate constants.

### Effect of pH on MXT degradation profile

The pH value of the drug solution was one of the most important parameters for the electro-Fenton process. In this study, the effect of reaction medium pH was investigated for each electrode and the drug concentration profile were monitored for pH = 3, 7 and 10. The results are depicted in Figure 5. It can be concluded that the removal rate became worse for pH > 3. As shown in Figure 5b, d and f, the kinetic constants of the CC electrode (0.0555), GO/CC electrode (0.0683) and  $\text{Fe}_3\text{O}_4@\text{GO}/\text{CC}$  electrode (0.154) are higher at pH 3 than other pHs. This distinguish that the removal rate at pH 3 is more than pH 7 and 10. This can be related to the low production of oxidizing  $\text{OH}^\bullet$  at these pHs while the optimum pH for the generation of

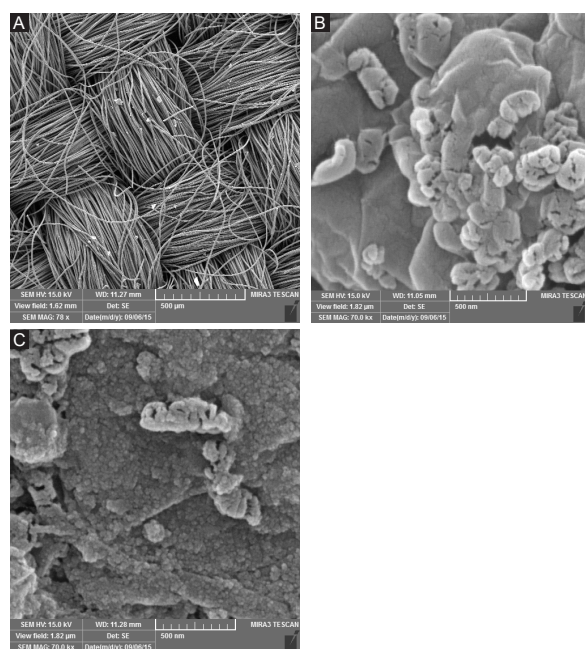


**Figure 2.** FE-SEM images of (A) CC (B) GO@CC (C)  $\text{Fe}_3\text{O}_4@\text{GO}/\text{CC}$  electrodes surface.

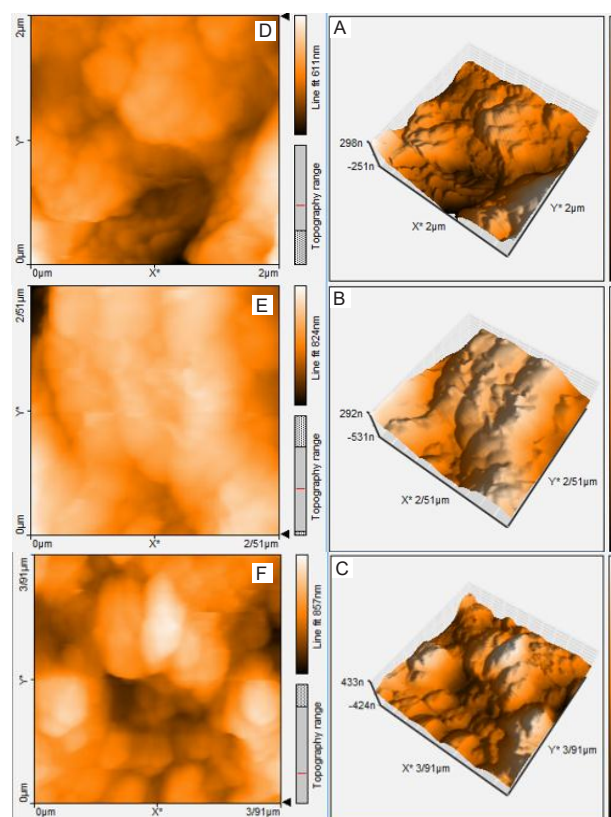


**Figure 3.** Three-dimensional AFM images of (A) CC, (B) GO@CC, (C)  $\text{Fe}_3\text{O}_4@\text{GO}/\text{CC}$ . Two-dimensional images of (D) CC, (E) GO@CC, (F)  $\text{Fe}_3\text{O}_4@\text{GO}/\text{CC}$ .

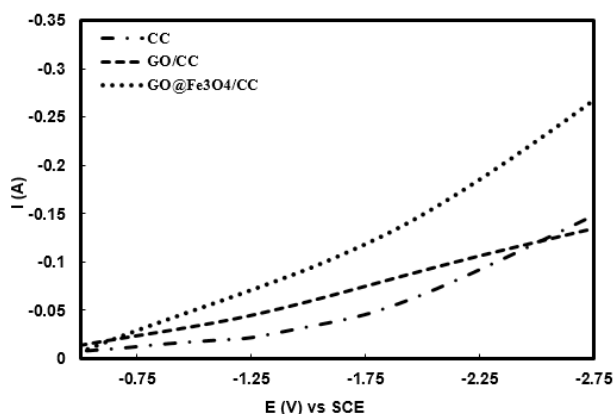


**Figure 4.** Cathode polarization curve of CC, GO@CC and  $\text{Fe}_3\text{O}_4@$ GO/CC in aqueous solution at pH 3.0 with air as atmosphere. Sweep rate =  $10 \text{ mVs}^{-1}$ ,  $[\text{Na}_2\text{SO}_4] = 0.05 \text{ M}$ , room temperature ( $25^\circ\text{C}$ ).

this radical is 2.8 (17, 31). A suitable pH facilitates  $\text{H}_2\text{O}_2$  formation and accelerates electro-Fenton reaction. On the

other hand, the kinetic constants at pH 3 shows that the removal rate increases in the following order:  $\text{Fe}_3\text{O}_4@$ GO/CC > GO/CC > CC. The highest extent of drug removal by the  $\text{Fe}_3\text{O}_4@$ GO/CC electrode was around 90% at pH 3 within 30 minutes of reaction.

Rosales et al (32) studied the electro-Fenton decoloration of dyes including Methyl Orange, Reactive Black 5 and fuchsin acid in a continuous reactor. They found that the optimum pH was 2.0 while the high pH ( $>3.0$ ) decreased the decoloration degree significantly, due to the lower dissolved fraction of iron species. In fact, at high pH values Fe(III) precipitates at high pH which reduces the dissolved Fe(III) concentration. Therefore, the concentration of Fe(II) species also decreases because Fe(III) hydroxides are much less reactive than dissolved Fe(III) species towards  $\text{H}_2\text{O}_2$ . Some studies reported that the lower pH ( $<3$ ) reduced the rate of the Fenton process owing to the reaction between Fe(III) and  $\text{H}_2\text{O}_2$  which inhibited the regeneration of Fe(II) (33,34). However, this

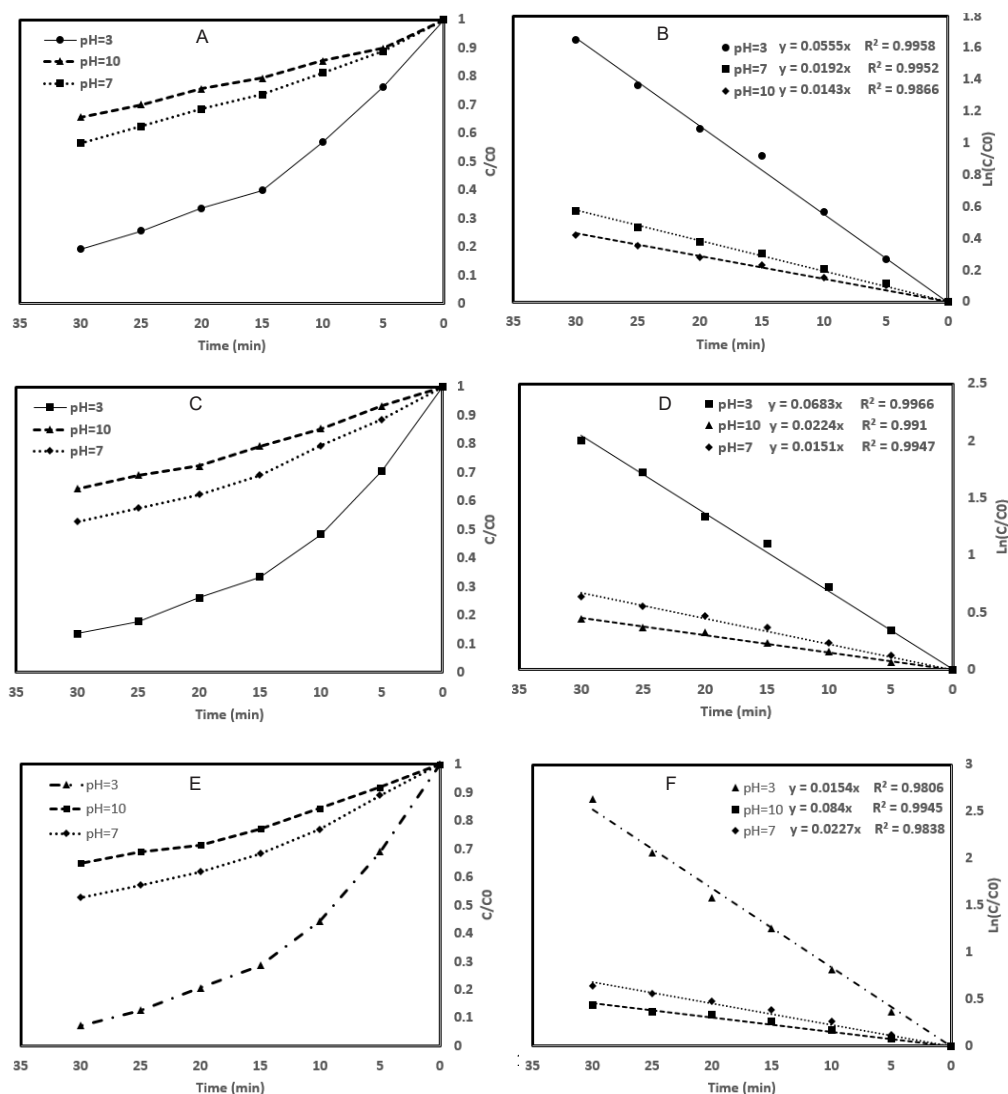


**Figure 5.** Degradation profile of MXT under different reaction medium pH by utilizing (A) CC electrode (C) GO/CC electrode (E)  $\text{Fe}_3\text{O}_4@$ GO/CC electrode (B, D, F) corresponding pseudo-first order kinetic lines of the data set respectively ( $C_0$ :  $5 \text{ mg/L}$ ,  $[\text{Na}_2\text{SO}_4]$ :  $0.05 \text{ M}$ ,  $V$ :  $200 \text{ mL}$ ,  $I = 100 \text{ mA}$ )

phenomenon did not happen through the electro-Fenton process because Fe(II) is continuously regenerated from the reduction of Fe(III) on the cathode surface (35).

#### Effect of electrical current intensity on MXT degradation

$H_2O_2$  is generated in situ by  $O_2$  reduction (Eq. 1) on the cathode in an electro-Fenton system and it is dependent on the applied current. In order to investigate the effect of electrical current intensity on the MXT degradation profile, different current intensities of 100, 200, 350 and 450 mA were utilized and the results are presented in Figure 6. It is clear that the increased current intensity enhanced the rate of MXT degradation. As it is clear in Figure 6b, d and f, when the applied current was increased from 100 to 450 mA, the rate constant of the pseudo-first order was increased from 0.0555 to 0.0845, 0.0683 to 0.1108 and 0.084 to 0.1282 on the CC electrode, GO/CC electrode and  $Fe_3O_4@GO/CC$  electrode state, respectively. This phenomenon can be related to the  $e^-$  role in Eqs.

(1-4) that the higher current intensity resulted in the higher generation rate of  $H_2O_2$  and  $Fe^{2+}$  and finally, the higher generation rate of  $OH^\bullet$  which resulted to the higher degradation rate (36). Since a higher voltage should be supplied to the system to reach a higher current intensity, the 100 mA was used in the following experiments as regards economical points. On the other hand, the kinetic constants at each current intensity increases in the following order:  $Fe_3O_4@GO/CC > GO/CC > CC$ . Annabi et al (37) studied the degradation of enoxacin antibiotic (ENO) by the electro-Fenton reaction using carbon-felt cathode and a platinum anode. The results showed that increasing the current intensity enhanced the ENO degradation yields. Hou et al (38) reported the heterogeneous electro-Fenton oxidation of catechol using nano- $Fe_3O_4$ . They found that the high current density ( $10 \text{ mA/cm}^2$ ) favored the high degradation efficiency (100%) within 120 minutes. Özcan et al (39) investigated the mineralization of norfloxacin (NFXN) from water through the electro-Fenton reaction.

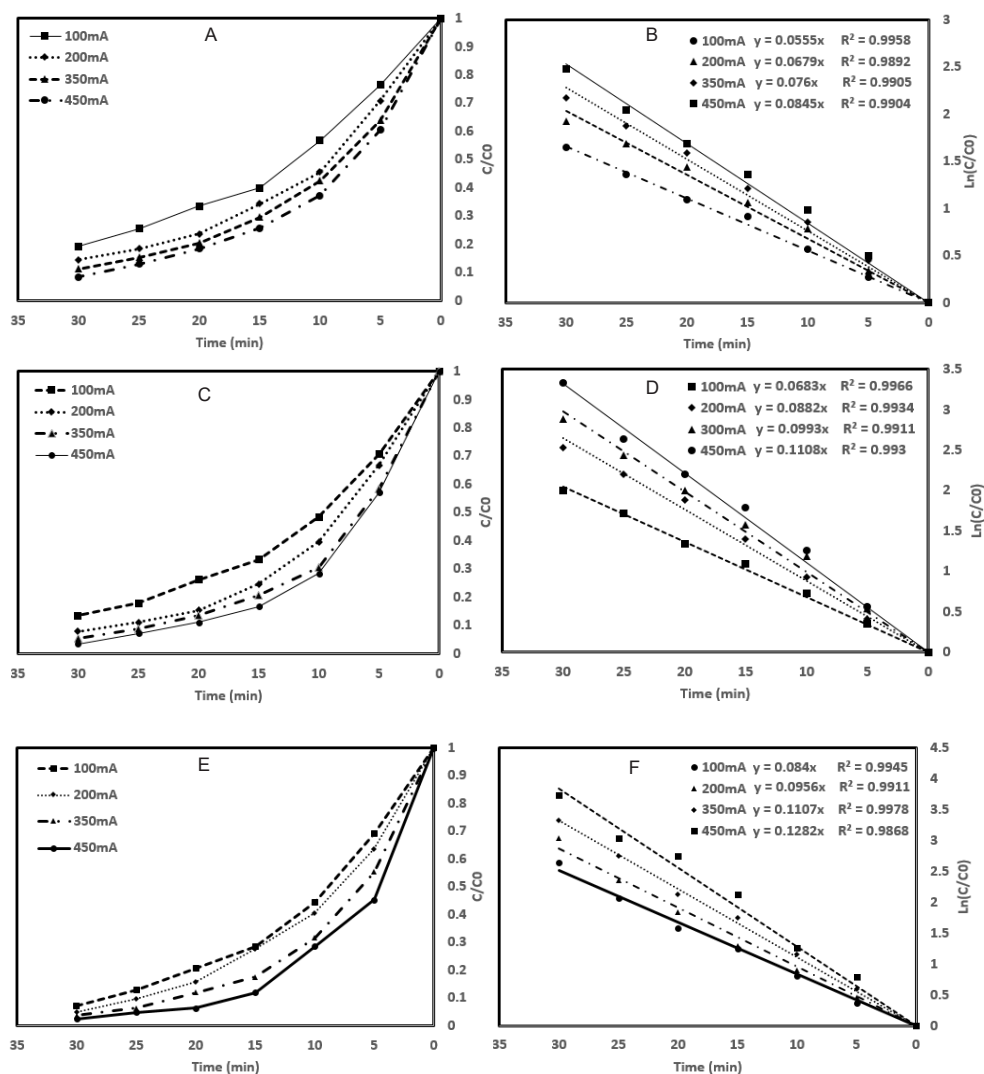


**Figure 6.** Degradation profile of MXT under different electrical current intensities (A) CC electrode (C) GO/CC electrode (E)  $Fe_3O_4@GO/CC$  electrode (B, D, F) corresponding pseudo-first order kinetic lines of the data set respectively ( $C_0$ : 5 mg/L,  $[Na_2SO_4]$ : 0.05 M, V: 200 mL, pH=3)

The results showed that increasing the current intensity up to 300 mA promoted the mineralization rate of NFXN while higher values (>300 mA) decreased the reaction rate.

### Effect of Fe catalyst concentration in homogenous electro-Fenton process

Different amounts of Fe catalyst (0.05, 0.1, 0.2 and 0.5 mM) provided different rate constants and different MXT degradation profiles (Figure 7). It could be seen that as Fe concentration increased after 0.2 mM, the degradation rate decreased due to the enhanced side reaction as follows:



As the  $Fe^{2+}$  concentration increased by the introduction of more Fe catalyst in the reaction medium, the side reaction rate increased and thus more hydroxyl was consumed. Consequently, the MXT degradation decreased because it was highly dependent on the hydroxyl concentration in the reaction medium (40,41). The process of the  $Fe_3O_4@GO/CC$  electrode was heterogeneous and thus, no amount of  $FeSO_4$  catalyst was dissolved in the reaction medium. Annabi et al (37) studied the effect of Fe(II) concentration on the degradation of ENO molecule in the presence of 50 mg/L ENO and an applied constant current intensity of 200 mA. An increase in the Fe(II) concentration up to 0.2 mmol/L increased the ENO degradation yields but it decreased above 0.2 mmol/L. This phenomenon can be attributed to the higher production of hydroxyl radicals by the high amount of Fe(II) based on the Fenton reaction (42). On the other hand, the negative effect of the higher Fe(II) concentration assigned to a competitive reaction

between the formed hydroxyl radicals and the excess of ferrous ions (42). Özcan et al (39) reported the similar effect of Fe(II) concentration in the mineralization of NFXN from water through the electro-Fenton reaction.

### Mineralization of MXT

The oxidizing power of the electro-Fenton method with different electrodes to mineralize the MXT solution was evaluated from the total organic carbon (TOC) decay. TOC decay measurements at pH=3, electrical current of 100 mA after 6 hours of electrolysis with the CC electrode, GO/CC electrode and 0.2 mM with Fe catalyst including  $Fe_3O_4@GO/CC$  electrode showed TOC removal as 82.8%, 86.1% and 96.9%, respectively.

### Conclusion

In this work, degradation of MXT drug in aqueous solution was performed by the electro-Fenton process using three different electrodes under various operational conditions. The electrochemical properties of electrodes were investigated and it can be concluded that the  $Fe_3O_4@GO/CC$  electrode released more current than the other two electrodes. The AFM results depicted more summits for the  $Fe_3O_4@GO/CC$  electrode which provided more active sites for producing  $H_2O_2$  and eventually, the higher MXT degradation rate. The kinetics of MXT degradation was obtained and well fitted to the pseudo-first order kinetics. It was concluded that the high pH of the reaction medium resulted in the low degradation rate. The higher current intensity provided the higher degradation rate. In a homogenous reaction, the results showed that

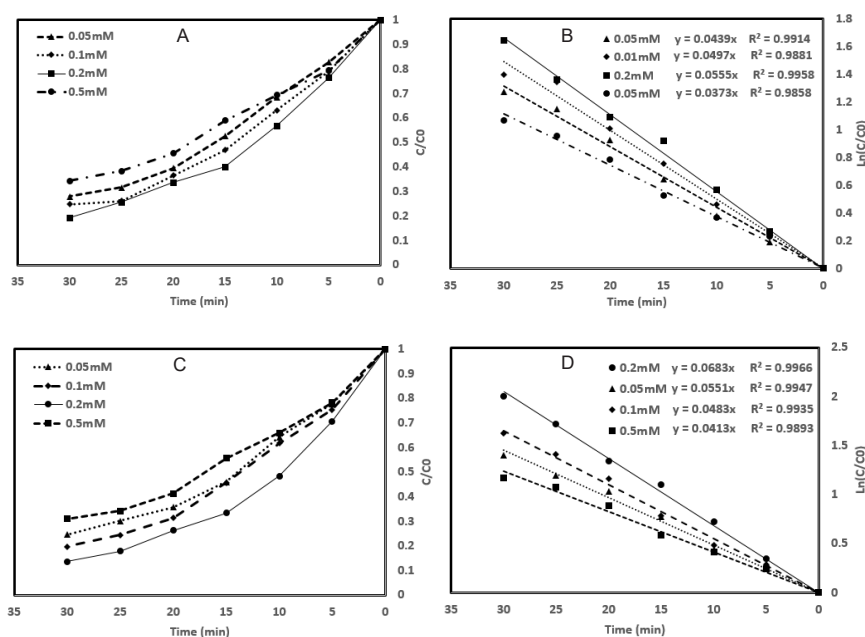


**Figure 7.** Degradation profile of MXT with different dissolved Fe catalyst in homogenous reaction (A) CC electrode (C) GO/CC electrode (B, D) corresponding pseudo-first order kinetic lines of the data set respectively ( $C_0$ : 5 mg/L,  $[Na_2SO_4]$ : 0.05M, V: 200 mL, pH=3, I = 100 mA).

after a certain amount of introduced Fe catalyst, the degradation rate decreased owing to the more wasted hydroxyl. In general, the heterogeneous electro-Fenton process included the advantage of reusable catalyst and electrode due to the lower catalyst lost compared with the homogenous process which would be a more suitable option in future works.

### Acknowledgements

The authors would like to thank the instrumental analysis lab of the department of chemical engineering of Sahand University of Technology for their assistance in the analysis and support for this study.

### Ethical issues

It is hereby declared that this work and the obtained results are the original experimental work of authors and it has neither been published, nor is it under review in another journal, and it is not being submitted for publication in any other journals.

### Competing interests

The authors declare that they have no competing interest.

### Authors' contributions

This work is the result of the full co-operation of all the mentioned authors.

### References

- Shaker S, Zafarian S, Chakra S, Rao KV, Badii K, Aftabtalab A, et al. Fabrication of Super Paramagnetic Nanoparticles by Sol-Gel Method for Water Purification. *Adv Mat Res* 2014; 829: 808-12. doi: 10.4028/www.scientific.net/AMR.829.808.
- Aftabtalab A, Sadabadi H. Application of magnetite (Fe<sub>3</sub>O<sub>4</sub>) nanoparticles in hexavalent chromium adsorption from aquatic solutions. *J Pet Environ Biotechnol* 2015; 6(200): 1-6. doi: 10.4172/2157-7463.1000200.
- Bendz D, Paxéus NA, Ginn TR, Loge FJ. Occurrence and fate of pharmaceutically active compounds in the environment, a case study: Höje River in Sweden. *J Hazard Mater* 2005; 122(3): 195-204. doi: 10.1016/j.jhazmat.2005.03.012.
- Ternes TA. Occurrence of drugs in German sewage treatment plants and rivers. Dedicated to Professor Dr. Klaus Haberer on the occasion of his 70th birthday. *Water Res* 1998; 32(11): 3245-60. doi: 10.1016/S0043-1354(98)00099-2.
- Lindqvist N, Tuhkanen T, Kronberg L. Occurrence of acidic pharmaceuticals in raw and treated sewages and in receiving waters. *Water Res* 2005; 39(11): 2219-28. doi: 10.1016/j.watres.2005.04.003.
- Hu J, Lo IM, Chen G. Comparative study of various magnetic nanoparticles for Cr(VI) removal. *Sep Purif Technol* 2007; 56(3): 249-56. doi: 10.1016/j.seppur.2007.02.009.
- Gholipour M, Hashemipour H, Mollashahi M. Hexavalent chromium removal from aqueous solution via adsorption on granular activated carbon: adsorption, desorption, modeling and simulation studies. *Journal of Engineering and Applied Sciences* 2011; 6(9): 10-8.
- Barakat MA. New trends in removing heavy metals from industrial wastewater. *Arabian Journal of Chemistry* 2011; 4(4): 361-77. doi: 10.1016/j.arabjc.2010.07.019.
- Mirbagheri SA, Hosseini SN. Pilot plant investigation on petrochemical wastewater treatment for the removal of copper and chromium with the objective of reuse. *Desalination* 2005; 171(1): 85-93. doi: 10.1016/j.desal.2004.03.022.
- Zarei M, Niaei A, Salari D, Khataee A. Application of response surface methodology for optimization of peroxi-coagulation of textile dye solution using carbon nanotube-PTFE cathode. *J Hazard Mater* 2010; 173(1-3): 544-51. doi: 10.1016/j.jhazmat.2009.08.120.
- Fatta-Kassinos D, Vasquez MI, Kummerer K. Transformation products of pharmaceuticals in surface waters and wastewater formed during photolysis and advanced oxidation processes - degradation, elucidation of byproducts and assessment of their biological potency. *Chemosphere* 2011; 85(5): 693-709. doi: 10.1016/j.chemosphere.2011.06.082.
- Klavarioti M, Mantzavinos D, Kassinos D. Removal of residual pharmaceuticals from aqueous systems by advanced oxidation processes. *Environ Int* 2009; 35(2): 402-17. doi: 10.1016/j.envint.2008.07.009.
- Sires I, Oturan N, Oturan MA. Electrochemical degradation of beta-blockers. Studies on single and multicomponent synthetic aqueous solutions. *Water Res* 2010; 44(10): 3109-20. doi: 10.1016/j.watres.2010.03.005.
- Khataee AR, Zarei M, Moradkhannejhad L. Application of response surface methodology for optimization of azo dye removal by oxalate catalyzed photoelectro-Fenton process using carbon nanotube-PTFE cathode. *Desalination* 2010; 258(1): 112-9. doi: 10.1016/j.desal.2010.03.028.
- Vosoughi M, Fatehifar E, Derafshi S, Rostamizadeh M. High efficient treatment of the petrochemical phenolic effluent using spent catalyst: Experimental and optimization. *J Environ Chem Eng* 2017; 5(2): 2024-31. doi: 10.1016/j.jece.2017.04.003.
- Rossmel J, Logadottir A, Nørskov JK. Electrolysis of water on (oxidized) metal surfaces. *Chemical Physics* 2005; 319(1-3): 178-84. doi: 10.1016/j.chemphys.2005.05.038.
- Shen J, Li Y, Zhu Y, Hu Y, Li C. Aerosol synthesis of Graphene-Fe<sub>3</sub>O<sub>4</sub> hollow hybrid microspheres for heterogeneous Fenton and electro-Fenton reaction. *J Environ Chem Eng* 2016; 4(2): 2469-76. doi: 10.1016/j.jece.2016.04.027.
- Zhao H, Wang Y, Wang Y, Cao T, Zhao G. Electro-Fenton oxidation of pesticides with a novel Fe<sub>3</sub>O<sub>4</sub>@Fe<sub>2</sub>O<sub>3</sub>/activated carbon aerogel cathode: High activity, wide pH range and catalytic mechanism. *Appl Catal B* 2012; 125: 120-7. doi: 10.1016/j.apcatb.2012.05.044.
- Ren W, Peng Q, Huang Za, Zhang Z, Zhan W, Lv K, et al. Effect of Pore Structure on the Electro-Fenton Activity of ACF@OMC Cathode. *Ind Eng Chem Res* 2015; 54(34): 8492-9. doi: 10.1021/acs.iecr.5b02139.
- Chen W, Yang X, Huang J, Zhu Y, Zhou Y, Yao Y, et al. Iron oxide containing graphene/carbon nanotube based carbon aerogel as an efficient E-Fenton cathode for the degradation of methyl blue. *Electrochim Acta* 2016; 200: 75-83. doi: 10.1016/j.electacta.2016.03.044.
- Hu X, Liu B, Deng Y, Chen H, Luo S, Sun C, et al.



- Adsorption and heterogeneous Fenton degradation of 17 $\alpha$ -methyltestosterone on nano Fe<sub>3</sub>O<sub>4</sub>/MWCNTs in aqueous solution. *Appl Catal B* 2011; 107(3-4): 274-83. doi: 10.1016/j.apcatb.2011.07.025.
22. Pereira MC, Oliveira LA, Murad E. Iron oxide catalysts: Fenton and Fenton-like reactions - a review. *Clay Miner* 2012; 47(3): 285-302. doi: 10.1180/claymin.2012.047.3.01.
  23. Ghandoor HE, Zidan HM, Khalil MM, Ismail MM. Synthesis and Some Physical Properties of Magnetite (Fe<sub>3</sub>O<sub>4</sub>) Nanoparticles. *Int J Electrochem Sci* 2012; 7(6): 5734-45.
  24. Shahriari T, Nabi Bidhendi G, Mehrdadi N, Torabian A. Effective parameters for the adsorption of chromium(III) onto iron oxide magnetic nanoparticle. *Int J Environ Sci Technol (Tehran)* 2014; 11(2): 349-56. doi: 10.1007/s13762-013-0315-z.
  25. Zhu Y, Murali S, Cai W, Li X, Suk JW, Potts JR, et al. Graphene and graphene oxide: synthesis, properties, and applications. *Adv Mater* 2010; 22(35): 3906-24. doi: 10.1002/adma.201001068.
  26. Porosoff MD, Yu W, Chen JG. Challenges and opportunities in correlating bimetallic model surfaces and supported catalysts. *J Catal* 2013; 308: 2-10. doi: 10.1016/j.jcat.2013.05.009.
  27. Zubir NA, Yacou C, Motuzas J, Zhang X, Diniz da Costa JC. Structural and functional investigation of graphene oxide-Fe<sub>3</sub>O<sub>4</sub> nanocomposites for the heterogeneous Fenton-like reaction. *Sci Rep* 2014; 4: 4594. doi: 10.1038/srep04594.
  28. Wang J, Tang B, Tsuzuki T, Liu Q, Hou X, Sun L. Synthesis, characterization and adsorption properties of superparamagnetic polystyrene/Fe<sub>3</sub>O<sub>4</sub>/graphene oxide. *Chem Eng J* 2012; 204(206): 258-63. doi: 10.1016/j.cej.2012.07.087.
  29. Chugun A, Uchide T, Tsurimaki C, Nagasawa H, Sasaki T, Ueno S, et al. Mechanisms responsible for reduced cardiotoxicity of mitoxantrone compared to doxorubicin examined in isolated guinea-pig heart preparations. *J Vet Med Sci* 2008; 70(3): 255-64.
  30. Manikas AC, Beobide AS, Voyiatzis GA. Quantitative analysis via Surface Enhanced Raman Scattering from Ag nano-colloids utilizing an oscillating cell and right-angle collection geometry. *Analyst* 2009; 134(3): 587-92. doi: 10.1039/b815053b.
  31. Wang X, Wang J, Guo P, Guo W, Wang C. Degradation of rhodamine B in aqueous solution by using swirling jet-induced cavitation combined with H<sub>2</sub>O<sub>2</sub>. *J Hazard Mater* 2009; 169(1-3): 486-91. doi: 10.1016/j.jhazmat.2009.03.122.
  32. Rosales E, Pazos M, Longo MA, Sanromán MA. Electro-Fenton decoloration of dyes in a continuous reactor: A promising technology in colored wastewater treatment. *Chem Eng J* 2009; 155(1-2): 62-7. doi: 10.1016/j.cej.2009.06.028.
  33. Ramirez JH, Duarte FM, Martins FG, Costa CA, Madeira LM. Modelling of the synthetic dye Orange II degradation using Fenton's reagent: From batch to continuous reactor operation. *Chem Eng J* 2009; 148(2): 394-404. doi: 10.1016/j.cej.2008.09.012.
  34. Pignatello JJ. Dark and photoassisted iron(3+)-catalyzed degradation of chlorophenoxy herbicides by hydrogen peroxide. *Environ Sci Technol* 1992; 26(5): 944-51. doi: 10.1021/es00029a012.
  35. Martínez-Huitle CA, Brillas E. Decontamination of wastewaters containing synthetic organic dyes by electrochemical methods: A general review. *Appl Catal B* 2009; 87(3-4): 105-45. doi: 10.1016/j.apcatb.2008.09.017.
  36. Su CC, Chang AT, Bellotindos LM, Lu MC. Degradation of acetaminophen by Fenton and electro-Fenton processes in aerator reactor. *Sep Purif Technol* 2012; 99: 8-13. doi: 10.1016/j.seppur.2012.07.004.
  37. Annabi C, Fourcade F, Soutrel I, Geneste F, Floner D, Bellakhal N, et al. Degradation of enoxacin antibiotic by the electro-Fenton process: Optimization, biodegradability improvement and degradation mechanism. *J Environ Manage* 2016; 165: 96-105. doi: 10.1016/j.jenvman.2015.09.018.
  38. Hou B, Han H, Jia S, Zhuang H, Xu P, Wang D. Heterogeneous electro-Fenton oxidation of catechol catalyzed by nano-Fe<sub>3</sub>O<sub>4</sub>: kinetics with the Fermi's equation. *Journal of the Taiwan Institute of Chemical Engineers* 2015; 56: 138-47. doi: 10.1016/j.jtice.2015.04.017.
  39. Özcan A, Atılır Özcan A, Demirci Y. Evaluation of mineralization kinetics and pathway of norfloxacin removal from water by electro-Fenton treatment. *Chem Eng J* 2016; 304: 518-26. doi: 10.1016/j.cej.2016.06.105.
  40. Borràs N, Arias C, Oliver R, Brillas E. Anodic oxidation, electro-Fenton and photoelectro-Fenton degradation of cyanazine using a boron-doped diamond anode and an oxygen-diffusion cathode. *J Electroanal Chem* 2013; 689: 158-67. doi: 10.1016/j.jelechem.2012.11.012.
  41. Feng L, Oturan N, van Hullebusch ED, Esposito G, Oturan MA. Degradation of anti-inflammatory drug ketoprofen by electro-oxidation: comparison of electro-Fenton and anodic oxidation processes. *Environ Sci Pollut Res Int* 2014; 21(14): 8406-16. doi: 10.1007/s11356-014-2774-2.
  42. Panizza M, Cerisola G. Electro-Fenton degradation of synthetic dyes. *Water Res* 2009; 43(2): 339-44. doi: 10.1016/j.watres.2008.10.028.